Time series of superconducting gravimeters and water storage variations from the global hydrology model WGHM

H. Wziontek, H. Wilmes, P. Wolf, S. Werth, A. Guntner

Accepted Manuscript

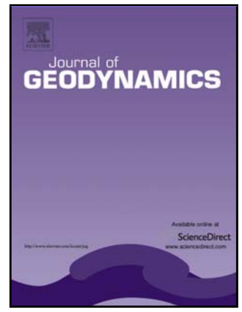

Title: Time series of superconducting gravimeters and water storage variations from the global hydrology model WGHM

Authors: H. Wziontek, H. Wilmes, P. Wolf, S. Werth, A. G¨untner

PII: S0264-3707(09)00103-3
DOI: doi:10.1016/j.jog.2009.09.036
Reference: GEOD 930

To appear in: *Journal of Geodynamics*

Time series of superconducting gravimeters and water storage variations from the global hydrology model WGHM

H. Wziontek[*,a], H. Wilmes[a], P. Wolf[a], S. Werth[b], A. Güntner[b]

[a]*Federal Agency for Cartography and Geodesy (BKG), Richard-Strauss-Allee 11, 60598 Frankfurt am Main, Germany*
[b]*Helmholtz Centre Potsdam, GFZ German Research Centre for Geosciences, Telegrafenberg, 14473 Potsdam, Germany*

Abstract

The gravimetric time series achieved from the combination of superconducting and absolute gravimeters are characterized by highest precision and long-term stability. If the effects of Earth and ocean tides, atmosphere and polar motion are removed, the residual curve is dominated by hydrological mass variations. A major source of these variations is water storage changes in the vicinity of the sensor. However, global variations contribute to the signal significantly. For three stations of superconducting gravimeters, a comparison of the principal components obtained from the residual gravity curve on the one hand and continental water storage from the WaterGAP Global Hydrological Model (WGHM) on the other hand is carried out. The results demonstrate a coherence of seasonal variations but a difference in the contribution of the local zone at the individual stations, which point out the need for a careful and site-specific examination of local effects.

Key words: gravimetry, superconducting gravimeter, water storage, global hydrology model

1. Introduction

Since several decades, starting with Bonatz (1967), it is well known, that besides atmospheric effects, water storage changes affect high precision gravimetric measurements significantly. While several proven methods exist to reduce atmospheric effects reaching from simple barometric admittance to three-dimensional modeling based on operational weather models (Warburton and Goodkind, 1977, Merriam, 1992, Kroner and Jentzsch, 1999, Neumeyer et al., 2004, Klügel and Wziontek, 2009), the contribution of hydrological variations is much more difficult to describe. Initially treated as a disturbing effect in the analysis of the Earth and ocean tides and the interpretation of long-term gravity changes, this signal is considered today as valuable information to quantify mass changes of the system Earth, to verify and improve models describing such processes or to supplement and validate other time-variable gravity field observations, e.g. results from the GRACE satellite mission (Neumeyer et al., 2008, Weise et al., 2009). Further on, the quantification of such mass variations is a prerequisite to infer height changes from gravity changes complementary to the results of geodetic space techniques.

Since the gravimeter is an integrating sensor, it is not possible to discriminate between different accelerating sources. Therefore, the analysis of a single effect presumes a sufficiently accurate modeling and elimination of all other relevant influences, which can be assumed for the main time-variable constituents originating from Earth and ocean tides, polar motion and atmospheric effects. By a comparison with the WaterGAP Global Hydrology Model (WGHM) (Döll et al., 2003) it will be examined, if variations visible in gravimetric time series of superconducting gravimeters (SG) are coherent with global and regional hydrological variations and a first estimate on the magnitude of site-specific local effects will be given.

2. Impact of hydrology induced mass effects on gravity

In general, hydrological mass variations are a global phenomenon and cause two effects, direct attraction according to Newton's law of gravitation and deformation due to the changing load on the Earth's surface. Since the magnitude of gravitational attraction diminishes with the square of the distance to the attracting masses, small variations in the vicinity of the sensor have a large impact on the observation. Although the gravimeter is only sensitive to the attraction component in vertical direction, mass changes in close vicinity of the sensor have considerable effect. In Creutzfeldt et al. (2008) it is demonstrated that up to 90% of the gravitational effect of a water layer with constant thickness located below topography over an area of several kilometers originates from sources within a distance of only a few 100 m around the computation point. Such influences will be denoted as local effects and arise primarily from changes in the local water storage. The area including all significant local gravity effects will be called near-zone. If this zone is divided into concentric

*Corresponding author
Email address: `hartmut.wziontek@bkg.bund.de` (H. Wziontek)

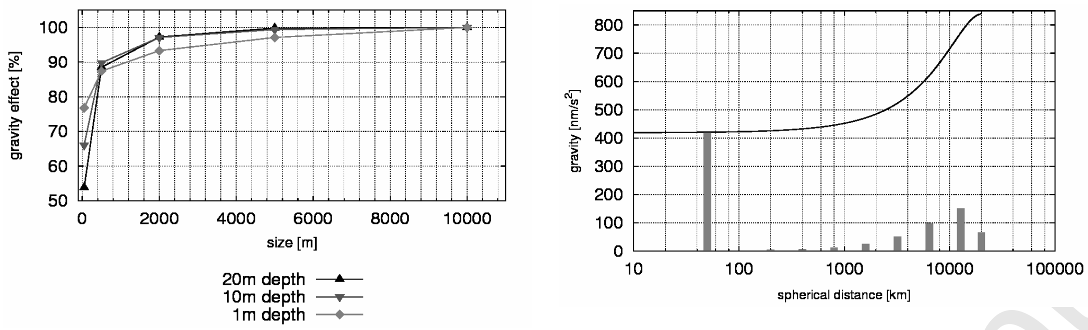

(a) Near-zone effect for different layer depths below topography

(b) Effect of spherical ring zones (bars) and cumulative effect (curve) for a point located 0.5 m above a spherical shell (R=6371 km)

Figure 1: Contribution of zones of different size to the gravitational effect induced by a water layer of 1 m thickness.

regions of increasing size around the computation point, the attraction effect for each region can be calculated by, e.g. an integration over elementary bodies, which yields a dependency on the size of the region as shown in figure 1(a).

To demonstrate the influence beyond this zone, a spherical shell[1] of water with constant thickness of 1 m was divided into spherical ring zones concentric to the point of computation. The attraction effect of each zone was calculated using the analytical expressions given in Heck and Seitz (2007) with respect to a point located close to the outer surface. Again, the main contribution results from the innermost zone which is almost equivalent to the effect of a Bouguer plate, since topography is neglected (Figure 1(b)). However, the remaining parts contribute significantly, doubling the entire effect, as already discussed by Vanícek et al. (2001). Therefore, the attraction effect should be considered in general as a global feature.

Deformation due to hydrological loads is primarily a global effect, as demonstrated by Llubes et al. (2004) for a homogeneous load, while for an inhomogeneous load distribution it tends more to be a regional feature, as will be discussed in section 4.

In conclusion, the calculation of gravity effects induced by hydrological mass changes will be divided into a near-zone up to a size of several kilometers and an outer zone to account for remaining parts of regional and global characteristics.

3. Gravimetric times series

The basis of this study is the time series from SGs operated by BKG at three central European stations. The registrations cover the period 2000-2007 for stations Wettzell (WE, Germany) and Medicina (MC, Italy) and 2002-2007 for station Bad Homburg (BH, Germany). As a common feature, these stations are located above ground. Most water storage changes take place below the gravimetric sensor, except for minor influences due to the surrounding topography or buildings.

The interpretation of small signals with annual amplitudes of 100 nm/s^2 and below calls for gravity time series of highest precision and long-term stability. The combination of records from SG with colocated absolute gravity measurements is the only terrestrial gravimetric technique to fulfill these requirements. After careful preprocessing (elimination of disturbances, steps and outliers), the method described in Wziontek et al. (2008) was used to determine zero reference drift and scale of all three SG as well as checks of the absolute gravimeters at all stations. A tidal analysis for constituents up to monthly tides of the Moon (*Mm*) was performed to model Earth tides after applying atmospheric corrections based on models of the German Weather Service (DWD) (Klügel and Wziontek, 2009) and reduction for polar motion. For comparison reasons, ocean tidal loading based on FES 2004[2] was removed further instead of analyzing the total tidal effect. The residual time series as shown in figure 2 are now assumed to be primarily characterized by hydrological variations. Despite a time shift, the curves for BH and MC show remarkable similarity in their seasonal patterns, while significant larger annual and inter-annual variations are visible at station WE.

4. Gravity effects from the WaterGAP Global Hydrology Model

The WaterGAP Global Hydrology Model (WGHM) (Döll et al., 2003) is a conceptual water balance model that simulates the continental water cycle at a spatial resolution of 0.5°. Water storage compartments represented in the model include interception, soil water, snow, groundwater and surface water (rivers, lakes, wetlands). WGHM

[1] or Bouguer shell

[2] using the ocean tide loading provider by M.S. Bos and H.-G. Scherneck: `http://www.oso.chalmers.se/~loading/`

has been widely used to analyze spatio-temporal variations of water storage globally and for large river basins (Güntner et al., 2007). In this study, the latest WGHM version as described in Hunger and Döll (2008) is used with model calibration against observed river runoff at 1235 discharge stations worldwide. WGHM is driven with monthly precipitation data from the Global Precipitation Climatology Centre (GPCC) (Rudolf and Schneider, 2004) and air temperature, radiation, and number of raindays within each month from the European Centre for Medium-Range Weather Forecast (ECWMF) operational forecasts.

For the period 2000-2007, direct attraction and loading effects induced by the mass changes from WGHM were calculated for the SG sites, adding the contribution of each individual model cell. Total water storage variations were used, except for the near-zone. Here, surface water changes from the relatively coarse model cannot be considered as representative for local attraction effects and were therefore excluded to avoid bias. Especially if the cell containing the computation point includes large streams like the river Po for station Medicina, this turned out to be important.

To compute the attraction effect, most of the cells can be represented simply by point masses, but in the vicinity of the computation point the spatial extent of the volume elements must be taken into account. Thus, the near-zone was approximated by a planar model and the gravitational effect of the respective cells was computed by integration over rectangular homogeneous prisms (Mader, 1951, Nagy, 1966, Forsberg, 1984), since topography was not incorporated in this first investigation. Tests showed that it is sufficient to include only WGHM cells within a radius of 50 km in the near-zone. As expected, the effect of the near-zone dominates the signal, but loading and global attraction contribute significantly (Figure 3).

The loading effect was calculated based on the well known Green's functions approach (Farrell, 1972) with coefficients given by Guo et al. (2004, table 2). The attraction part contributes globally with large variations in

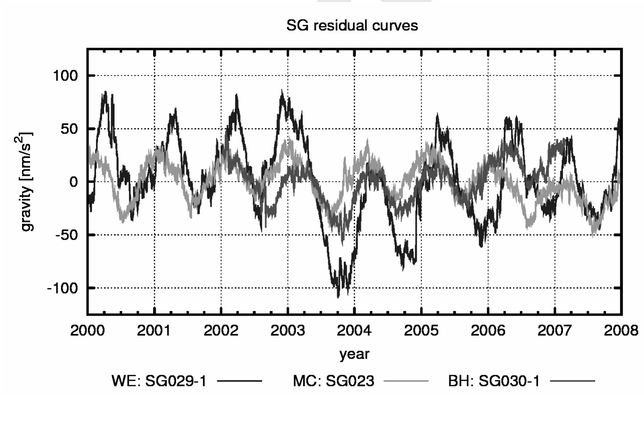

Figure 2: Residual gravity time series for stations Bad Homburg (BH) in dark grey, Medicina (MC) in light grey and Wettzell (WE) in black for the period 2000-2007.

the contribution of individual regions (Figure 4). Far distant masses may contribute even with opposite signs (Figure 4(b)). A significant difference of up to 4 nm/s^2 arises if cells beyond a radius of 1000 km are omitted, which underlines the necessity of a global computation. The main loading effect is generated by masses in the range of 50 to 3000 km and decreases rapidly for farther distances (Figure 4(c), 4(d)). While the magnitude changes with time, the distribution across the sections is preserved. Due to the irregular coverage of hydrological masses, this distribution is noticeably different from the load of a homogenous

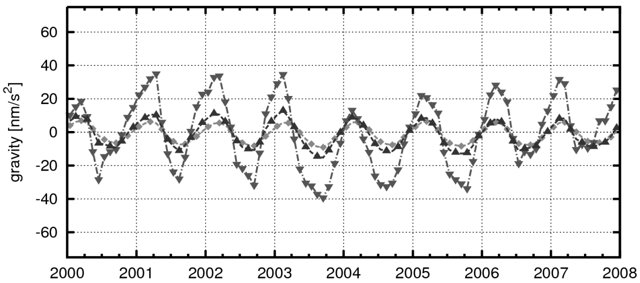

(a) Bad Homburg (BH)

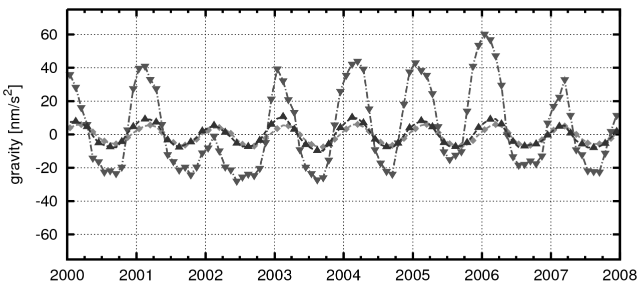

(b) Medicina (MC)

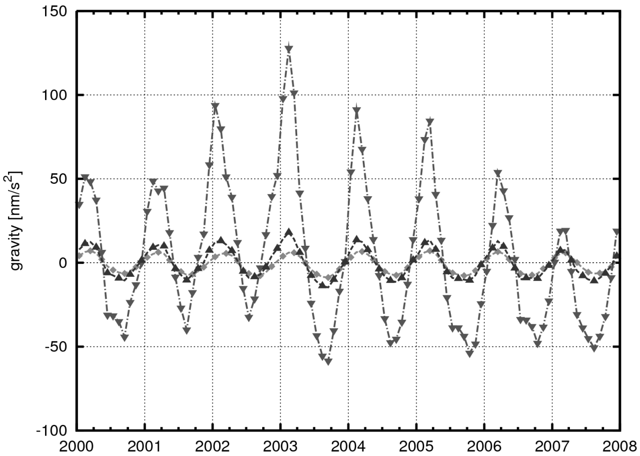

(c) Wettzell (WE)

Figure 3: Gravity effects due to water mass variations from WGHM resulting from Newtonian attraction in the near-zone (dot-dashed line, reversed triangles), in remaining global continental cells (dotted line, upright triangles) and from deformation (grey line, diamonds) for the period 2000-2007.

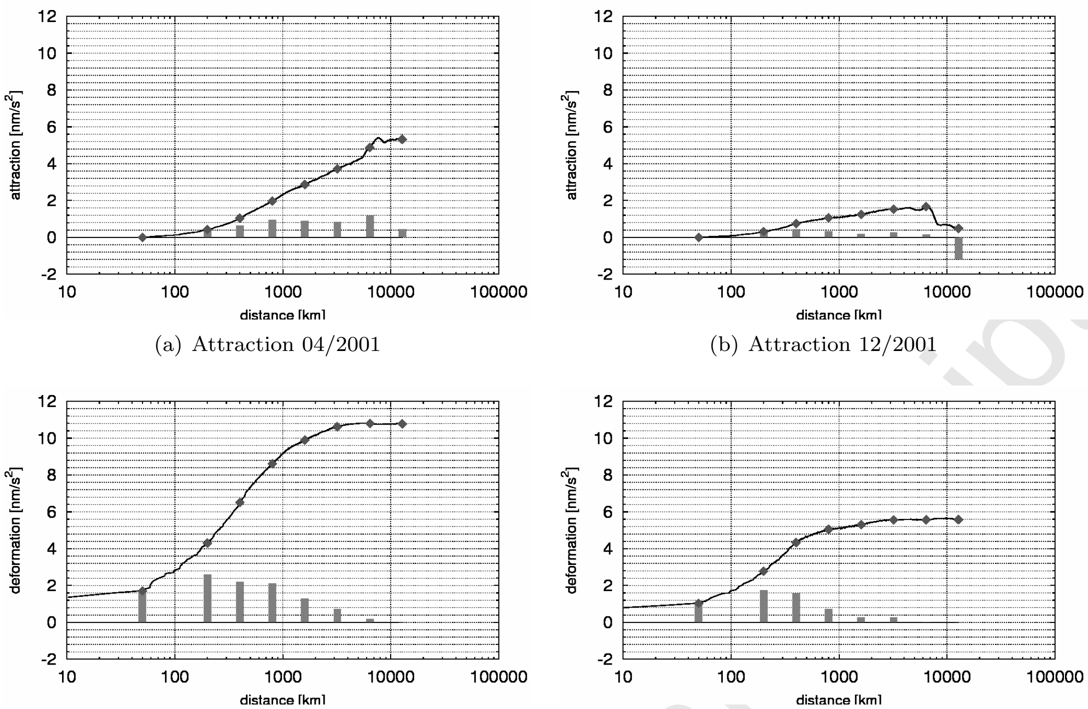

(a) Attraction 04/2001 (b) Attraction 12/2001

(c) Loading 04/2001 (d) Loading 12/2001

Figure 4: Effects of gravitational attraction of the outer zone and loading effect as obtained from WGHM in relation to distance from point of computation (in km) for station Bad Homburg (BH). Displayed are the contribution of individual regions (bars) and the cumulative effect (curve).

layer as given in Llubes et al. (2004).

Although the global effects are quite similar for all three stations, the near-zone attraction effect shows considerably more singular behaviour for the different stations. This can be attributed to the site-specific meteorological and hydrological conditions at each station (Figure 3).

5. Comparison of modeled gravity signal with residual time series from SG

To compare the gravity effect resulting from the previous section with the SG residual time series, the different temporal and spatial resolution has to be considered. While WGHM gives monthly mean values on a grid size of roughly 50 km, SG time series are available with a sampling rate of 5 min as point observations. Obviously, a generalization of the SG residual curve is needed for comparison. Singular spectrum analysis (SSA), an approach based on principal component analysis (PCA) applied in the time domain was used (Vautard and Ghil, 1989, Vautard et al., 1992, Golyandina et al., 2001). The time series is decomposed with a window into a sequence of lagged vectors which form a trajectory matrix. Its eigenvectors are called temporal empirical orthogonal functions (EOF). Projection of the time series onto each EOF yields the corresponding temporal principal components (PC). The four main components were used to reconstruct the signal. The results are presented in figure 5 together with the gravity effects of the outer zone and the total effect (including the near-zone) computed from WGHM. Table 1 characterizes the mean annual variability obtained by stacking the respective gravity effects shown in figure 5 over an annual period.

Besides a general similarity of the annual component of both, SG and WGHM series, it is obvious that for stations BH and MC the total effect markedly exceeds the amplitude of the SG registration, whereas for station WE this is not the case (Table 1 and Figure 5). In contrast, the sum of the global attraction and loading effects agrees well with the time series at stations BH and MC, but does not explain the gravity variations at WE. One reason could be, that at the stations BH and MC, only minor local effects are observable by the SG due to specific environmental conditions.

Station BH is situated in a mainly sealed and well drained urban area on a rock of green schist near to the Taunus mountain ridge. A very low pore volume of the bedrock with nearly no fissures in conjunction with the well drained or sealed surrounding area might cause only little water storage changes within the radius of influence of attraction effects of the near-zone

Station MC is located in the Po river plain with intensive agricultural use in its vicinity. It can be assumed, that irrigation and drainage of the neighbouring farmland alters or compensates largely natural changes in the local

Table 1: Mean annual variability of gravity effects computed from WGHM and the reconstructed residual time series for SG-Stations based on principal components 1–4 for stations Wettzell (WE), Bad Homburg (BH) and Medicina (ME) in nm/s^2.

	attraction near-zone			attraction global			deformation			SG (PC 1-4)		
	WE	BH	MC	WE	BH	MC	WE	BH	MC	WE	BH	MC
min	-34	-33	-32	-7	-7	-6	-10	-11	-8	-46	-23	-23
max	62	36	36	6	6	5	12	10	8	53	18	25
var	96	69	68	13	13	12	22	21	15	99	40	47
rms	34	24	25	5	5	4	8	8	6	33	14	15

water storage. As a further indication for missing local variations, the unusually low precipitation in that region

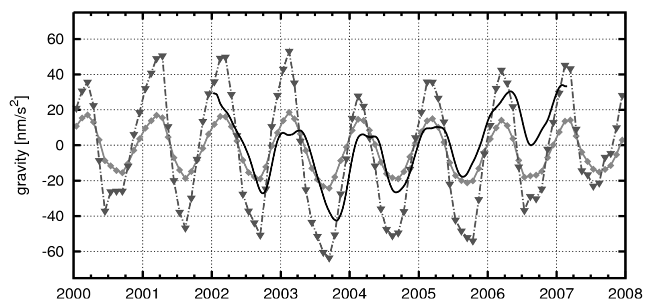

(a) Bad Homburg (BH)

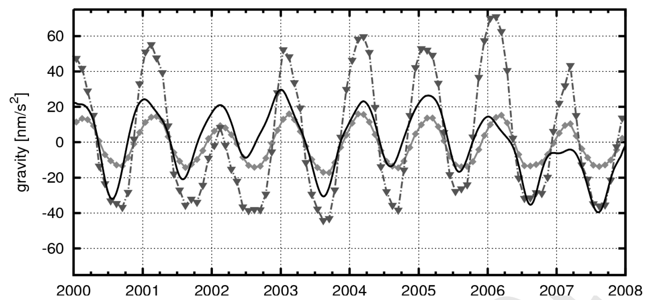

(b) Medicina (MC)

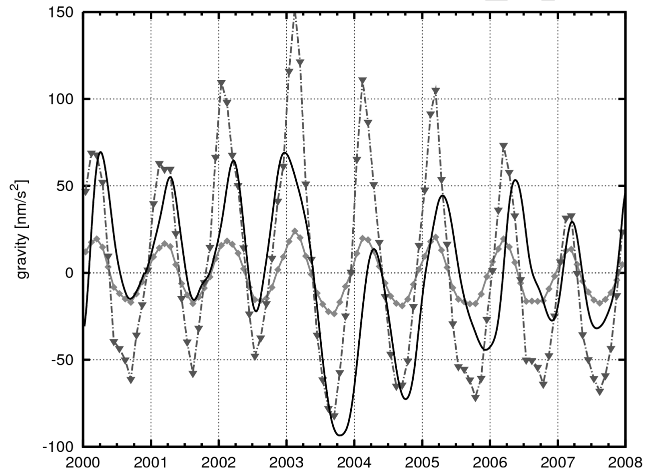

(c) Wettzell (WE)

Figure 5: Gravity effects of water mass variations from WGHM due to attraction and loading including (dot-dashed line, reversed triangles) and excluding (grey line, diamonds) the near-zone compared with generalized SG records (black line) for the period 2000-2007.

during the winter 2001/2002 can be identified clearly in WGHM, but is not visible in the SG registration.

In contrast, station WE is located on a ridge in the lower mountain range of the Bavarian Forest with a complex local geological structure, but with little anthropogenic influences. Here, the total effect agrees fairly well with the SG residual curve and suggests an overlap of local and global hydrological variations. Especially the large gravity decrease after the dry summer 2003 is present in both curves with comparable amount. In the consecutive period of 3 years only the SG has observed a slow increase in gravity, most likely linked to regeneration of the local water storage. Since in a mountainous region a significant influence of topography is expected, differences may partly be explained if a terrain model is included in the analysis (Creutzfeldt et al., 2008).

In addition, it should be noted that due to the coarse resolution and uncertainties of the global hydrological model applied here, data of water storage variations of the WGHM cells around the SG stations will not fully represent the real hydrological variations close to the SGs. WGHM gives averaged data for the region from which water mass variations in the near-zone may differ due to small-scale heterogeneities in geological, soil and vegetation characteristics.

The different correlation of the SG records with global or total effects reflects the complexity of the interaction between water storage changes and the gravity effect. Especially the strong dependency on the respective SG site, even if located above ground, clearly demonstrates the need of detailed investigations in the vicinity of the stations.

6. Conclusions

SG registrations at three stations in central Europe were compared with the WaterGAP Global Hydrology Model (WGHM) by a computation the gravity effect of water storage changes. The innermost zone close to the gravimeter was included by integration over rectangular homogeneous prisms. By this means, global as well as local contributions to the signal were assessed. It is concluded, that the contribution of hydrology in the local zone is site-dependent. Whereas for station Wettzell a good agreement with the total SG signal could be stated, the gravity time series at Medicina and Bad Homburg coincide only with the global effects (attraction and loading). Most likely, the environmental characteristics of these stations prevent natural water storage changes within the radius of strong gravitational sensitivity, which has to be supported by local hydrological measurements in future studies. The results clearly demonstrate the need for a site-specific quantification of local water storage changes.

Acknowledgment. The authors thank C. Kroner, GFZ German Research Centre for Geosciences Potsdam, Germany for comparison of numerical results, and V. Pálinkáš, Research Institute of Geodesy, Topography and Cartography, Geodetic Observatory Pecný, Czech Republic for fruitful discussions. We acknowledge J. Alcamo and P. Döll for providing the WGHM model code. The work was supported by the Deutsche Forschungsgemeinschaft (DFG) in the frame of the Priority Research Program 1257 "Mass Transport and Mass Distribution in the Earth System" (NE 1409/1-1, KR 1906/8-1, IH 19/4-1).

References

Bonatz, M., 1967. Der Gravitationseinfluß der Bodenfeuchtigkeit. Zeitschrift für Vermessungswesen 92 (4), 135–139.

Creutzfeldt, B., Güntner, A., Klügel, T., Wziontek, H., 2008. Simulating the influence of water storage changes on the superconducting gravimeter of the Geodetic Observatory Wettzell, Germany. Geophysics 73 (6), WA95–WA104.

Döll, P., Kaspar, F., Lehner, B., 2003. A global hydrological model for deriving water availability indicators: model tuning and validation. Journal of Hydrology 270 (1-2), 105–134.

Farrell, W. E., 1972. Deformation of the Earth by Surface Loads. Reviews of Geophysics and Spaces Physics 10 (3), 761–797.

Forsberg, R., 1984. A Study of Terrain Reductions, Density Anomalies and Geophysical Inversion Methods in Gravity Field Modelling. Reports of the Department of Geodetic Science and Surveying 355, Ohio State University.

Golyandina, N., Nekrutkin, V., Zhigleiiavskiai, A. A., 2001. Analysis of Time Series Structure: SSA and Related Techniques. Chapman and Hall.

Güntner, A., Stuck, J., Werth, S., Döll, P., Verzano, K., Merz, B., 2007. A global analysis of temporal and spatial variations in continental water storage. Water Resources Research 43, W05416.

Guo, J. Y., Li, Y. B., Huang, Y., Deng, H. T., Xu, S. Q., Ning, J. S., 2004. Green's function of the deformation fo the Earth as a result of atmospheric loading. Geophysical Journal International 159 (1), 53–68.

Heck, B., Seitz, K., 2007. A comparison of the tesseroid, prism and point-mass approaches for mass reductions in gravity field modelling. Journal of Geodesy 81, 121–136.

Hunger, M., Döll, P., 2008. Value of river discharge data for global-scale hydrological modeling. Hydrology and Earth System Sciences 12 (3), 841–861.

Klügel, T., Wziontek, H., 2009. Correcting gravimeters and tiltmeters for atmospheric mass attraction using operational weather models. Journal of Geodynamics (this issue).

Kroner, C., Jentzsch, G., 1999. Comparison of different barometric pressure reductions for gravity data and resulting consequences. Physics of the Earth and Planetary Interiors 115, 205–218.

Llubes, M., Florsch, N., Hinderer, J., Longuevergne, L., Amalvict, M., 2004. Local hydrology, the Global Geodynamics Project and CHAMP/GRACE perspective: some case studies. Journal of Geodynamics 38, 355–374.

Mader, K., 1951. Das Newtonsche Raumpotential prismatischer Körper und seine Ableitungen bis zur dritten Ordnung. Österreichische Zeitschrift für Vermessungswesen Sonderheft 11.

Merriam, J. B., 1992. Atmospheric pressure and gravity. Geophysical Journal International 109, 488–500.

Nagy, D., 1966. The gravitational attraction of a right rectangular prism. Geophysics 31, 362–371.

Neumeyer, J., Barthelmes, F., Kroner, C., Petrovic, S., Schmidt, R., Virtanen, H., Wilmes, H., 2008. Analysis of gravity field variations derived from Superconducting Gravimeter recordings, the GRACE satellite and hydrological models at selected European sites. Earth Planets Space 60, 505–518.

Neumeyer, J., Hagedoorn, J., Leitloff, J., Schmidt, T., 2004. Gravity reduction with three-dimensional atmospheric pressure data for precise ground gravity measurements. Journal of Geodynamics 38, 437–450.

Petrović, S., 1996. Determination of the potential of homogeneous polyhedral bodies using line integrals. Journal of Geodesy 71, 44–52.

Rudolf, B., Schneider, U., 2004. Calculation of gridded precipitation data for the global land-surface using in-situ gauge observations. In: Proceedings of the 2nd Workshop of the International Precipitation Working Group IPWG, Monterey, October 2004. pp. 231–247.

Vanícek, P., Novák, P., Martinec, Z., 2001. Geoid, topography, and the Bouguer plate or shell. Journal of Geodesy 75 (4), 210–215.

Vautard, R., Ghil, M., 1989. Singular spectrum analysis in nonlinear dynamics, with applications to paleoclimatic time series. Physica D 35, 395–424.

Vautard, R., Yiou, P., Ghil, M., 1992. Singular-spectrum analysis: A toolkit for short, noisy chaotic signals. Physica D 58, 95–126.

Warburton, R. J., Goodkind, J. M., 1977. The influence of barometric-pressure variations on gravity. Geophysical Journal of the Royal Astronomical Society 48, 281–292.

Weise, A., Kroner, C., Abe, M., Ihde, J., Jentzsch, G., Naujoks, M., Wilmes, H., Wziontek, H., 2009. Terrestrial gravity observations with superconducting gravimeters for validation of satellite-derived (grace) gravity variations. Journal of Geodynamics (this issue).

Wziontek, H., Falk, R., Wilmes, H., Wolf, P., 2008. Precise gravity time series and instrumental properties from combination of superconducting and absolute gravity measurements. In: Sideris, M. (Ed.), Observing our Changing Earth. Vol. 133 of International Association of Geodesy Symposia. Springer, Berlin Heidelberg, pp. 301–306.